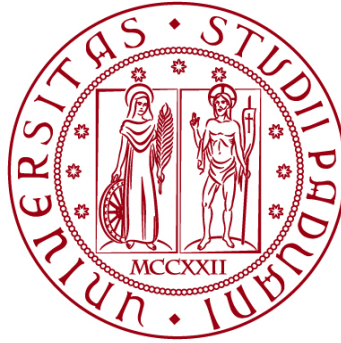


**UNIVERSITÀ DEGLI STUDI DI PADOVA**

DIPARTIMENTO DI BIOLOGIA  
Corso di Laurea in Biotecnologie



**ELABORATO DI LAUREA**

# Role of the cGAS-STING pathway in CIK cell therapy

**Tutor: Dott.ssa Roberta Sommaggio**

**Dipartimento di Scienze Chirurgiche Oncologiche e Gastroenterologiche**

**Laureando: Andrea Della Fazia**

**ANNO ACCADEMICO 2022/2023**

# INDEX

<b>1</b>	<b>ABSTRACT.....</b>	<b>1</b>
<b>2</b>	<b>INTRODUCTION .....</b>	<b>2</b>
2.1	Adoptive cell therapy and its applications .....	2
2.2	Cytokine Induced Killer (CIK) cells.....	2
2.3	The cGAS-STING pathway.....	3
2.3.1	cGAS-STING pathway activation and regulation .....	3
2.3.2	Activation of the cGAS-STING pathway in cancer cells.....	4
	<b>AIM OF THE STUDY .....</b>	<b>6</b>
<b>3</b>	<b>MATERIALS AND METHODS .....</b>	<b>7</b>
3.1	Cell lines and culture .....	7
3.2	PBMCs extraction from buffy coats .....	7
3.3	Expansion of Cytokine-induced killer (CIK) cells .....	7
3.4	Expansion of MCF-7 cells .....	8
3.5	Treatment of MCF-7 cells with ADU-S100 .....	8
3.6	Flow cytometry .....	9
3.6.1	CIK cells.....	10
3.6.2	MCF-7 cells.....	10
3.7	Calcein-acetoxymethyl (AM) assay .....	10
<b>4</b>	<b>RESULTS.....</b>	<b>12</b>
4.1	CIK cells' phenotypic characterization.....	12
4.1.1	CIK cells' gating strategy.....	12
4.1.2	CIK cells' phenotype .....	13
4.2	MCF-7 cells' phenotypic characterization.....	14
4.2.1	MCF-7 cells' gating strategy .....	14
4.2.2	MCF-7 cells' phenotype .....	15
4.3	Cytotoxic activity of CIK cells .....	16
4.3.1	Trastuzumab-mediated CIK cell retargeting .....	17
<b>5</b>	<b>DISCUSSION AND CONCLUSIONS.....</b>	<b>19</b>
	<b>REFERENCES .....</b>	<b>21</b>

## 1 ABSTRACT

The cyclic GMP-AMP synthase-stimulator of interferon genes (cGAS-STING) pathway is an innate immune response activated by the sensing of cytosolic double-stranded DNA. The activation of the pathway leads to the expression of pro-inflammatory cytokines which trigger the activation of the immune system. Previous studies have demonstrated that the activation of the cGAS-STING pathway in cancer cells promotes antitumor immunity and increases the survival time of the patient by inducing cancer cells' senescence and apoptosis and enhancing the infiltration of immune cells in the tumor microenvironment. Since cancer cells evolved to avoid the activation of the cGAS-STING pathway we tried to stimulate its activation via the treatment of MCF-7 breast cancer cells with ADU-S100, a STING agonist, to see whether it would lead to the activation of the pathway and to a consequent increase in the antitumor activity of adoptive CIK cells treatment. MCF-7 cells' phenotype was obtained via flow cytometry and the cytotoxic activity of CIK cells against the target was assessed through a calcein-AM cytotoxic assay. We demonstrated that the treatment of MCF-7 breast cancer cells with different concentrations of ADU-S100 leads to an increase in the surface expression of multiple NKG2D ligands thus increasing CIK cells' antitumor activity.

## 2 INTRODUCTION

### 2.1 Adoptive cell therapy and its applications

Adoptive cell therapy (ACT), also known as cellular immunotherapy, refers to a wide group of treatments that utilize our immune cells to cure different diseases, such as cancer. Our immune system can recognize and kill infected, damaged, and also cancerous cells. The concept behind adoptive cell therapy is to enhance the activity and efficiency of our immune system so that it becomes able to better individuate and eradicate cancer cells. There are different approaches to ACT and, while some of them involve the isolation of autologous immune cells followed by *in vitro* expansion and activation, such as Tumor Infiltrating Lymphocytes (TILs), Natural Killer cells (NK), Cytokine-Induced Killer (CIK) cells; others involve their genetic modification to enhance their ability to recognize and eliminate cancer cells, such as engineered T Cell Receptor (TCR) or Chimeric Antigen Receptor (CAR) T cells (Cancer Research Institute, 2023).

### 2.2 Cytokine Induced Killer (CIK) cells

Cytokine-induced killer (CIK) cells are a heterogeneous population of immune effector cells featuring a mixed T- and Natural Killer (NK) cell-like phenotype due to the surface expression of both CD3<sup>+</sup> and CD56<sup>+</sup> (Schmeel et al., 2014). They can be obtained by *ex vivo* expansion of Peripheral Blood Mononuclear Cells (PBMCs) with Interferon  $\gamma$  (IFN- $\gamma$ ), OKT3 (anti-CD3 monoclonal Antibody), and IL-2. CD3 is a transmembrane protein complex located on the surface of T cells and associated with the T-cell receptor (TCR), its role is to activate both T cytotoxic and T helper cells. CD56 (NCAM, neural cell adhesion molecule) is a glycoprotein that can be found on the surface of different cell lines, including NK cells and activated CD8<sup>+</sup> T cells. CIK cells are being used as a therapeutic agent against both solid and hematological tumors. The cytotoxicity against tumoral cells is MHC-unrestricted and is mediated by the NKG2D receptor (Figure. 1). NKG2D is a transmembrane activating receptor with the ability to bind at least 6 ligands, including MHC I-like molecules, MICA and MICB (MHC class I related proteins), and different members of the ULBP family (stress-induced proteins). Interestingly, these ligands are usually expressed in malignant tissues while their expression is almost absent in healthy tissues. Different studies suggested that the cytotoxic effect of CIK cells is mediated by the interaction between NKG2D and its ligand rather than TCR engagement (Introna, 2017). The fact that these cells present MHC-unrestricted cytotoxicity is extremely important because malignant cells are often not susceptible to MHC-restricted interactions due to mutations causing the inability to expose tumor antigens. Moreover, it has been demonstrated that CIK cells are

not cytotoxic against healthy cells, making its applicability effective in the treatment of different types of malignancies (Introna, 2017).

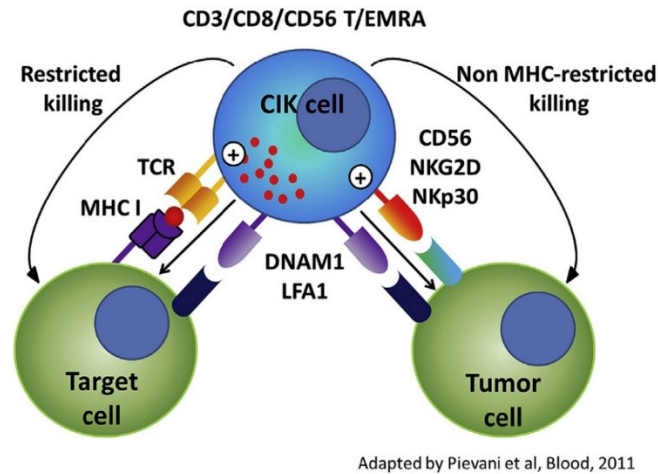


**Fig. 1. “Double T/NK specificity of CIK cells and their mechanism of action”.** CIK cells originate from T-EMRA lymphocytes which acquire NK-like cytotoxicity. DNAM1 and LFA1 are always required for target binding while CD56, NKp30, and NKG2D molecules mediate NK-like cytotoxicity. (Introna, 2017)

## 2.3 The cGAS-STING pathway

### 2.3.1 cGAS-STING pathway activation and regulation

The cyclic GMP-AMP synthase-stimulator of interferon genes (cGAS-STING) pathway is an innate immune response activated by the sensing of cytosolic double-stranded DNA via both cGAS and STING. The presence of dsDNA in the cytosol is not physiological and it usually stands for a microbial or a viral infection, but it can also be found in tumor cells. The interaction between cytosolic dsDNA and cGAS induces conformational changes in cGAS which lead to its activation and, therefore, to the initiation of the cGAS-STING signal transduction cascade. Activated cGAS produces cGAMP (cyclic GMP-AMP), a second messenger which binds and activates the stimulator of interferon genes (STING) dimer. STING dimers promote the recruitment of TBK1 (TANK-Binding Kinase 1), IRF3 (Interferon Regulatory Factor 3), and the activation of NF- $\kappa$ B (nuclear factor-kappaB). TBK1 phosphorylates both STING and IRF3. Afterward, both IRF3 and NF- $\kappa$ B are transported inside the nucleus where they stimulate the transcription of IFN-I and other cytokines, such as TNF, IL-1 $\beta$ , and IL-6 (Du et al., 2021). The increase in the expression of IFN-I and other pro-inflammatory cytokines triggers the maturation and antigen presentation of DCs, thereby linking innate immune responses to adaptive immune responses (Chen et al., 2016).

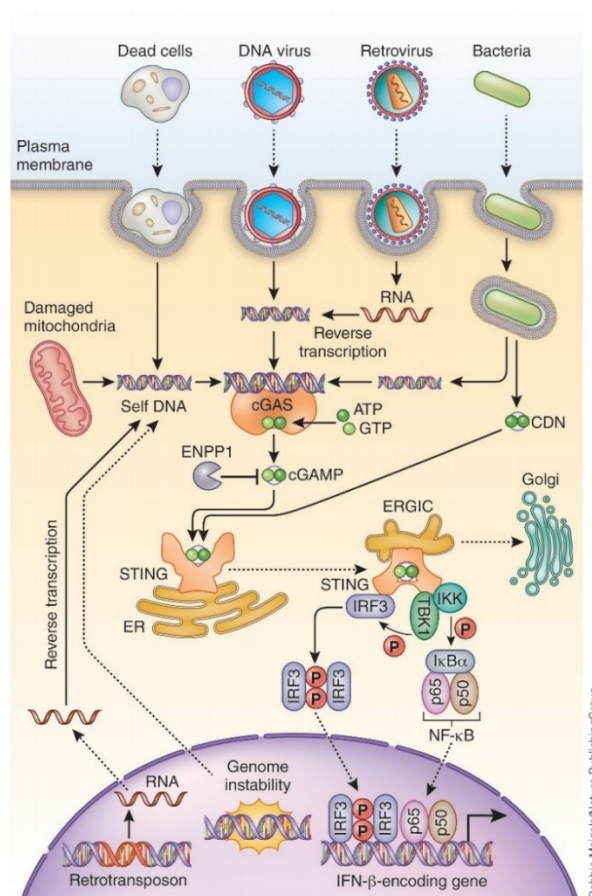


**Fig. 2. “The cGAS-STING pathway of cytosolic DNA sensing”.** DNA can be both a PAMP (Pathogen Associated Molecular Pattern) and a DAMP (Damage Associated Molecular Pattern). The figure describes the different steps of the cGAS-STING signal transduction cascade (Chen et al., 2016).

### 2.3.2 Activation of the cGAS-STING pathway in cancer cells

Cancer cells usually present chromosomal abnormalities or genomic DNA damage due to their high proliferation rate and consequent genomic instability. These dsDNA fragments can activate cGAS in a cellular autonomic way, thus triggering the activation of the cGAS-STING pathway which leads to the production of IFN-I and other pro-inflammatory cytokines that stimulate cancer cells' senescence and apoptosis, improve adaptive anticancer immunity, and inhibit or eliminate cancer cells (Du et al., 2021). Furthermore, different clinical studies showed that lower STING expression is associated with reduced survival time in patients with different cancers, including gastric cancer and lung adenocarcinoma. These findings encouraged further research on the relationship between STING agonists and cancer. The concept behind the treatment of cancer cells with different STING agonists, such as ADU-S100 (c-di-AMP analog), is to induce the activation of the cGAS-STING pathway resulting in the release of IFN-I and pro-inflammatory

cytokines by cancer cells. Furthermore, STING agonists also increase the expression of NKG2D ligands on the surface of the cancerous cell, thus enhancing NK cells infiltration in the tumor microenvironment (TME) and increasing their cytotoxic activity against transformed cells (Bert et al., 2014). The release of IFN-I and the other pro-inflammatory cytokines enhances DCs maturation, CD8<sup>+</sup> T-cells activation and induces the expression of multiple ligands, such as ULBP1 and ULBP3, which can promote NK cells infiltration in the TME, followed by recognition and elimination of cancerous cells through the release of perforin and granzyme (Esteves et al., 2021). One of the main issues related to the chronic stimulation of the cGAS-STING pathway induced by the administration of STING agonists is that the constant inflammatory state might promote inflammation-driven tumorigenesis. This is one of the reasons why it is fundamental to determine the optimal STING agonist level to guarantee the induction of a proper antitumor immune response while avoiding inflammation-induced tumorigenesis. Furthermore, it has been demonstrated that different cancers can evolve to destroy the cGAS signal pathway in order to bypass cGAS-STING-mediated immune surveillance (Du et al., 2021). Natural Killer (NK) cells and T cells are thought to be the main effectors of cancer immune surveillance. DNA fragments released from tumor cells exist in the tumor microenvironment and they can be absorbed by dendritic cells (DCs) activating the cGAS-STING pathway which leads to IFN-I production and, therefore, the induction of DCs maturation. Mature DCs stimulate CD8<sup>+</sup> T-cell activation thus enhancing tumor-specific T-cell responses. Furthermore, the release of cytokines caused by cGAS-STING activation in tumor cells leads to an increase in NK cell infiltration in the tumor microenvironment. NK cells present MHC-unrestricted cytotoxicity and can directly recognize and eliminate infected or cancerous cells through the secretion of cytokines, thus triggering an adaptive immune response (Du et al., 2021). NK cells feature NKG2D, a cellular receptor that recognizes different ligands, such as ULBP1, ULBP3, or ULBP4-5-6, interestingly these ligands are only expressed in malignant tissues thus making NK cells able to selectively kill only cancer cells without damaging healthy tissues. This ability joined with the fact that CIK cells can be easily obtained and expanded *in vitro* made them one of the most promising therapies for the treatment of both solid and hematological tumors.

## AIM OF THE STUDY

In this study, we will treat a breast cancer cell line (MCF-7) with ADU-S100, a c-di-AMP analog, and a STING agonist, to upregulate the expression of NKG2D's ligands, such as MIC-A, MIC-B, and multiple members of the ULBP family thus increasing CIK-mediated recognition and elimination of cancer cells. In addition, since CIK cells also express CD16a (Cappuzzello et al., 2016), we evaluated the effectiveness of the combination between CIK cells and Trastuzumab on the antitumor activity of CIK cells following the activation of antibody-dependent cellular cytotoxicity (ADCC).



## 3 MATERIALS AND METHODS

### 3.1 Cell lines and culture

MCF-7 (Michigan Cancer Foundation-7, ATCC) breast cancer cell line was cultured in Dulbecco's Modified Eagle Medium (DMEM) growth medium (Euroclone) in treated Falcon T25 flasks. CIK cells were cultured in Roswell Park Memorial Institute (RPMI) 1640 (Euroclone). Both RPMI-1640 and DMEM media were supplemented with 10% FBS (heat-inactivated fetal bovine serum) (Gibco), 1% Penicillin/Streptomycin (Euroclone), 1% HEPES buffer (Euroclone) and 1% U-glutamine (Euroclone) in order to obtain the complete medium (cRPMI-1640 and cDMEM).

### 3.2 PBMCs extraction from buffy coats

The buffy coat is the fraction of the anticoagulated blood sample that includes the majority of white blood cells and platelets, it is obtained after the centrifugation of the whole blood. PBMCs were extracted from buffy coats obtained by healthy donors, the blood was both provided and tested by the hospital of Padua. PBMCs were isolated through the use of a Lymphoprep (density: 1.077 g/mL) (Alere Technologies) density gradient centrifugation. The blood bag was cleaned with 70% ethanol and mixed thoroughly before being processed. 12.5 mL of buffy coat were transferred in a 50 mL Falcon tube and diluted 1:1 with 1X D-PBS (Sigma-Aldrich). 12.5 mL of Lymphoprep were aliquoted in a different 50 mL Falcon tube. The D-PBS-blood solution was slowly poured on the Lymphoprep to stratify it. The sample was then centrifuged at 1800 RPM for 20' at room temperature (RT) without breaks in order to avoid the disruption of the separation. After the centrifugation, the PBMC ring located above the Lymphoprep solution was harvested without touching the red blood cells located at the bottom of the tube. The cells were washed twice in D-PBS and then suspended in cRPMI-1640. PBMCs were counted using a Burker chamber and Trypan blue solution (Sigma-Aldrich), a dye that can enter non-viable cells thus staining them blue and allowing the counting and the evaluation of the cells' vitality.

### 3.3 Expansion of Cytokine-induced killer (CIK) cells

PBMCs were seeded at day 0 to the final density of  $5 \times 10^6$  cells/mL in 10 mL of cRPMI-1640 in a T25 non-treated flask (Falcon) and supplemented with 1000 U/mL of recombinant human interferon- $\gamma$  (hIFN- $\gamma$ , RnD system) to stimulate their proliferation. The flask was then incubated at 37°C and 5% CO<sub>2</sub>. After 24 hours 500

U/mL of recombinant human interleukin 2 (rhIL-2, Proleukin) and 50 ng/mL of anti-CD3 mAb (OKT3, Miltenyi Biotec, clone OKT3) were added.

The cells were passaged every 3-4 days (days 4, 7, 11, and 14 according to Figure. 3) at the density of  $1.5 \times 10^6$  cells/mL in a total volume of 13.3 mL of cRPMI-1640. In order to passage CIK cells,  $20 \times 10^6$  cells were collected in a 14 mL tube and centrifuged at 1300 RPM for 5' at RT. The pellet was then resuspended in 13.3 mL of cRPMI-1640 and supplemented with 500 U/mL of rhIL-2. The flasks were then incubated at 37°C and 5% CO<sub>2</sub>. Cell number and vitality were assessed by counting the cells in the sample with a Burker chamber and Trypan blue.

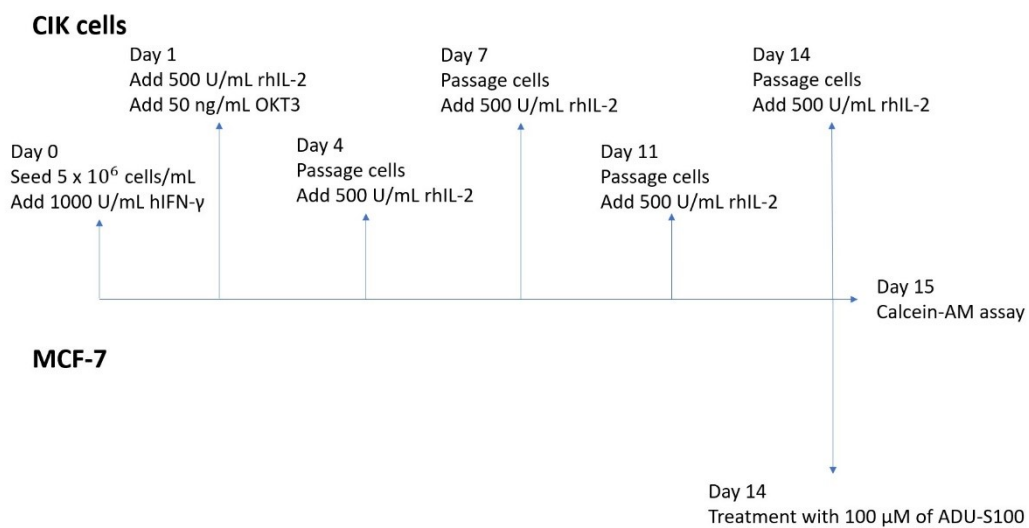


**Fig. 3. Passage of CIK cells.** This timeline sums up the experimental procedure used to expand CIK cells

### 3.4 Expansion of MCF-7 cells

MCF-7 breast cancer cells were cultured in complete DMEM medium in T25-treated flasks. The cells were passaged 1:3 when their confluence was around 70-80%. If confluent, MCF-7 cells were detached from the flask with 1 mL of Trypsin (Gibco) and then incubated at 37°C and 5% CO<sub>2</sub> for 5'. The trypsinization process was inhibited by the addition of cDMEM medium which can inactivate trypsin due to the presence of FBS in the medium. MCF-7 cells were passaged 1:3 in 7 mL of cDMEM and supplemented with 1  $\mu$ g/mL of insulin (Sigma-Aldrich). The cells were cultured in the incubator at 37°C and 5% CO<sub>2</sub>.

### 3.5 Treatment of MCF-7 cells with ADU-S100

MCF-7 cells were treated with different concentrations of ADU-S100 (0, 1, 5, 25, and 100  $\mu$ M) for 24, 48, and 72 hours. Briefly,  $3 \times 10^5$  cells were seeded in a 24-wells plate (Thermofisher) and incubated for 24 hours to allow them to attach to

the plate. The day after, the medium was removed and replaced with a new medium containing different concentrations of ADU-S100. The cells were then incubated at 37°C and 5% CO<sub>2</sub>. The cells were harvested by trypsinization 24, 48, and 72 hours after the treatment and their phenotype was analyzed by flow cytometry. To perform the calcein assay 5 x 10<sup>5</sup> MCF-7 cells were seeded in a 6-well plate (Thermofisher). 24 hours after, the cells were treated with 100 μM of ADU-S100 for 24 hours. After the treatment, the cells were harvested by trypsinization to characterize their phenotype and to perform the calcein-AM assay.

### 3.6 Flow cytometry

Flow cytometry is a technique used to detect and measure both physical and chemical features of a population of cells. In this study, both MCF-7 and CIK cells were stained with different fluorophore-conjugated monoclonal antibodies (mAbs) to characterize their phenotype.

Singlets were gated through an FSC-A vs FSC-H plot in which the height and the area of the pulse were compared to gate singlets and remove clumps from the analysis. It is fundamental to remove the clumps of cells from the analysis because flow cytometry is based on single cells analysis, not on doublets or clumps of cells analysis. Usually, in the case of clumps of cells, the transit time through the flow cytometer increases leading to an increase in the area of the pulse. Single cells fall along a diagonal line showing a linear relationship between the area and the height of the pulse while clumps of cells will show up with increased area relative to the height. Single cells were also gated via an FSC-A vs FSC-W plot in which the area and the width of the pulse were compared to isolate single cells. Viable cells were gated with Fixable Viability Stain 780 dye (FVS780, BD Bioscience). Fluorophore-conjugated FVS780 labels non-viable cells, which were identified by their fluorescence and then excluded from the analysis, thus gating viable cells.

Lymphocytes were gated through an FSC-A vs SSC-A plot which allows the identification of specific cells' populations based on the analysis of their relative size and complexity. The different populations in the bulk sample were gated via the analysis of the expression of specific surface markers, whose expression was assessed by the use of fluorophore-conjugated mAbs. This process allowed the gating of NK cells (CD56<sup>+</sup>/CD3<sup>-</sup>), T-cells (CD3<sup>+</sup>/CD56<sup>-</sup>), and CIK cells (CD3<sup>+</sup>/CD56<sup>+</sup>). The expression of NKG2D, CD8, CD4, and CD16 on the surface of CIK cells was assessed via multiple SSC-A vs specific-fluorescence plots as shown in Figure 6.

The same procedure was used to gate the target MCF-7 cell population, the only difference was that other mAbs were used to characterize their phenotype.

A Celesta flow cytometer was used to perform the FCM, while the results were read with DIVA software (BD Biosciences). Data analysis was performed using FlowJo (Treestar).

### 3.6.1 CIK cells

CIK cells' phenotype was obtained by flow cytometry.  $0.1-1 \times 10^6$  cells were collected into FCM tubes and diluted with 1-2 mL of D-PBS. The tubes were then centrifuged at 1300 RPM for 5' at RT. CIK cells were stained with CD3-BV510 (clone UCHT1, Biolegend), CD56-PE (clone HCD56, Biolegend), CD4-BV650 (clone SK3, BD Horizon), CD8-BV421 (clone RPA-T8, BD Horizon), CD16-FITC (clone 3G8, Biolegend), and NKG2D-APC (clone 1D11, Biolegend). The staining buffer was made of Brilliant staining buffer (BD Bioscience) and D-PBS 1%. The viability of CIK cells was assessed by Fixable Viability Stain 780 dye (FVS780). The cells were stained in the dark for 30' at 4°C. After the staining, the tubes were washed with 1-2 mL of D-PBS and then centrifugated. The supernatant was discarded to remove the mAbs in excess. CIK cells were then suspended in 300  $\mu$ L of D-PBS and analyzed with BD FACSCelesta Cell Analyzer (BD Biosciences).

### 3.6.2 MCF-7 cells

MCF-7 phenotype was obtained by flow cytometry. At least  $1 \times 10^5$  ADU-S100 treated MCF-7 cells were harvested with trypsin, as mentioned before. The cells were washed with D-PBS and then centrifuged to collect the cellular pellet. MCF-7 cells were stained with ULBP2/5/6-PerCP (R&D, clone 165931), ULBP1-Alexa488 (R&D, clone 170818), ULBP3-APC (R&D, clone 166510), MICA A/B-PE (R&D, clone 159207) and then incubated in the dark for 30' at 4°C. After the incubation, FCM tubes were washed again in D-PBS to remove the excess of mAbs. The cellular pellet obtained after the centrifugation was resuspended in 200  $\mu$ L of D-PBS and analyzed with BD FACSCelesta Cell Analyzer (BD Biosciences).

## 3.7 Calcein-acetoxymethyl (AM) assay

The calcein-acetoxymethyl (AM) assay is based on the use of a non-fluorescent calcein derivate (calcein-AM). This molecule can be internalized by viable cells, thus staining them. Inside viable cells, endogenous esterases can convert calcein-AM into green-fluorescent calcein by hydrolysis, this process can happen only in live cells since it requires cellular activity. While calcein-AM is a lipophilic molecule, calcein itself is a polar molecule that remains in the cytoplasm and cannot leak outside the cell. If the target cell is lysed by the effector calcein is released and it can be detected in the supernatant by a fluorimetric measurement.

MCF-7 cells were split 1:2 into 2 different T25 flasks the day before the calcein-AM assay to ensure that they are in the growing phase on the day of the assay. On the day of the assay, MCF-7 cells were seeded at a density of  $0.5 \times 10^6$  cells/well in a

6-well plate for 24h to let the cells attach to the plate. After 24h, the cells were treated with 100  $\mu$ M ADU-S100. After an additional 24 hours of ADU-S100 treatment, MCF-7 cells were stained with 3.5  $\mu$ M calcein-AM (EMD Millipore Corporation) in 5 mL of cRPMI-1640, and then incubated at 37°C for 30'. After the staining, 5 mL of D-PBS were added to the tubes which were then centrifuged at 1300 RPM for 5' at RT to obtain the stained cellular pellet. 2000 mCF-7 target cells were cocultured with CIK cells at different effector-target ratios (E:T) through a serial dilution in a 96-well U-bottom plate. The final E:T ratios were 50:1, 25:1, 12.5:1, 6.25:1, 3.125:1, and 1.56:1 in a final volume of 200  $\mu$ L of cRPMI-1640. The plate was incubated at 37°C and 5% CO<sub>2</sub> for 6 hours. In addition, 1  $\mu$ g/mL of Trastuzumab (Roche), an anti-HER-2 monoclonal antibody, was added into the coculture to exploit the consequences of the activation of the ADCC process in the cytotoxic activity of CIK cells towards MCF-7 cell line. 1  $\mu$ g/mL of Rituximab (Roche), an anti-CD19 mAb, was used to measure CIK cells' basal killing level, as a control. The maximum release of calcein by MCF-7 cells was assessed by the use of a Tryton 3% solution (prepared in cRPMI). The spontaneous release was evaluated via MCF-7 cells cultured in cRPMI-1640 only, without effector cells. After the incubation, the plates were centrifuged at 1300 RPM for 3' at RT and 100  $\mu$ L of supernatant were transferred to a black 96-well plate (Perkin Elmer). The plates were read using a VictorX4 Nivo™ (Perkin Elmer) plate reader. The specific lysis was calculated as follows:

$$\% \text{ specific lysis} = \frac{\text{experimental release} - \text{spontaneous release}}{\text{maximum release} - \text{spontaneous release}} \times 100$$

## 4 RESULTS

### 4.1 CIK cells' phenotypic characterization

#### 4.1.1 CIK cells' gating strategy

Each blood sample was characterized by flow cytometry to identify the percentage of viable CIK cells and to quantify the levels of expression of the surface markers of interest. The background signal, produced by the presence of auto-fluorescent cells that can trigger the laser, thus altering the phenotypic characterization, was isolated using an unstained tube. Singlets were isolated as stated in the material and methods and used to analyze the cells of interest. The isolation of single cells showed that *in vitro* cultured cells were highly viable, with over 90% of vitality. The lymphocyte population was isolated and characterized via the analysis of their specific size (FSC, Forward Scatter) and granularity (SSC, Side Scatter). The cultured PBMC population was highly pure with over 90% of the cells being identified as lymphocytes. Different cell subpopulations were then isolated via the analysis of specific surface markers (CD3 and CD56), as shown in Figure. 4.

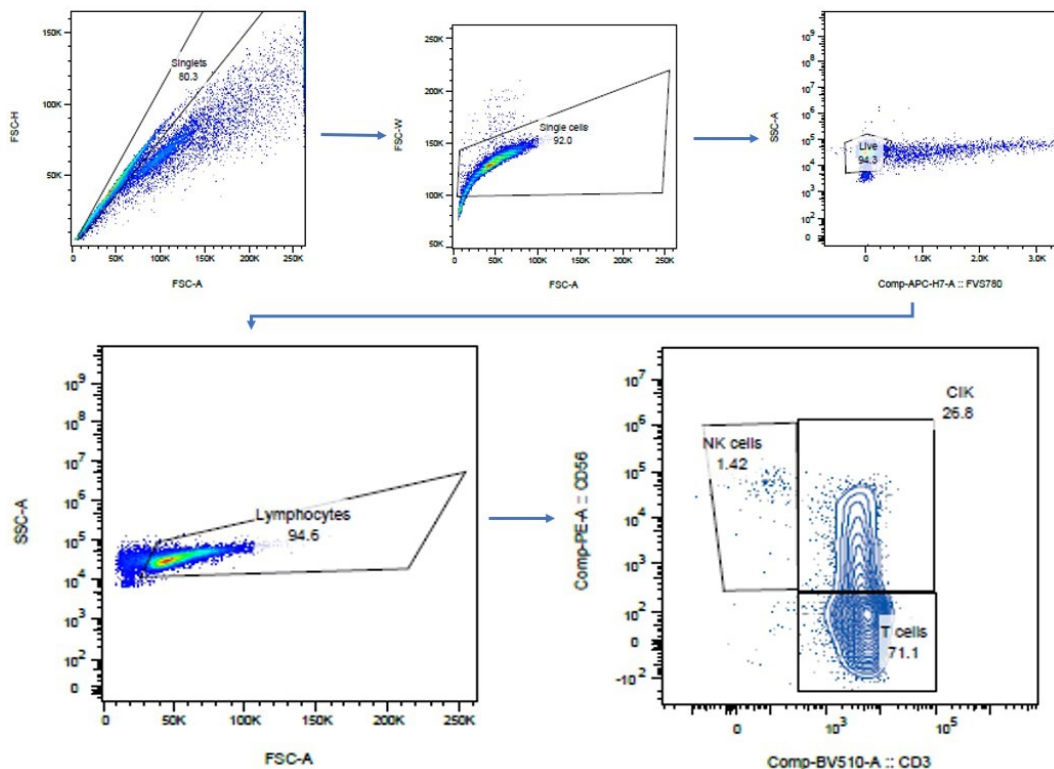


**Fig. 4. Gating of CIK cells in the sample.** The image shows the gating procedure used to isolate CIK cells (only one representative donor is shown).

#### 4.1.2 CIK cells' phenotype

The analysis of the isolated lymphocyte population after 14 days of culture showed that its composition varied among different donors. The double positive CD3<sup>+</sup> / CD56<sup>+</sup> CIK cells population was present at different percentages ranging from 25,4% to 30,1% (mean: 27,4 ± 2,41%) (Fig. 5). NKG2D expression on the surface of CIK cells was very high, ranging from 91,6% to 97,5% (mean: 95,1 ± 3,08%). The flow cytometry showed that also CD8<sup>+</sup> cytotoxic T-cells were highly present in the culture, indeed, CD8 expression ranged from 83.9% to 97.0 % (mean: 89,5 ± 6,77%). A minor subpopulation of CD4<sup>+</sup> T-cells was also found in the samples. CD4 expression varied between donors ranging from 5.93% to 27.3% (mean: 14.9 ± 11,1%). In addition, a small fraction of CIK cells (0.49% to 3.29%, mean: 1.50 ± 1.55%) expressed CD16a, which is a surface marker usually found on the membrane of NK cells and one of the main mediators of ADCC (Fig.7). Since the distribution of the different cellular populations varied between donors we assumed its donor-dependency.

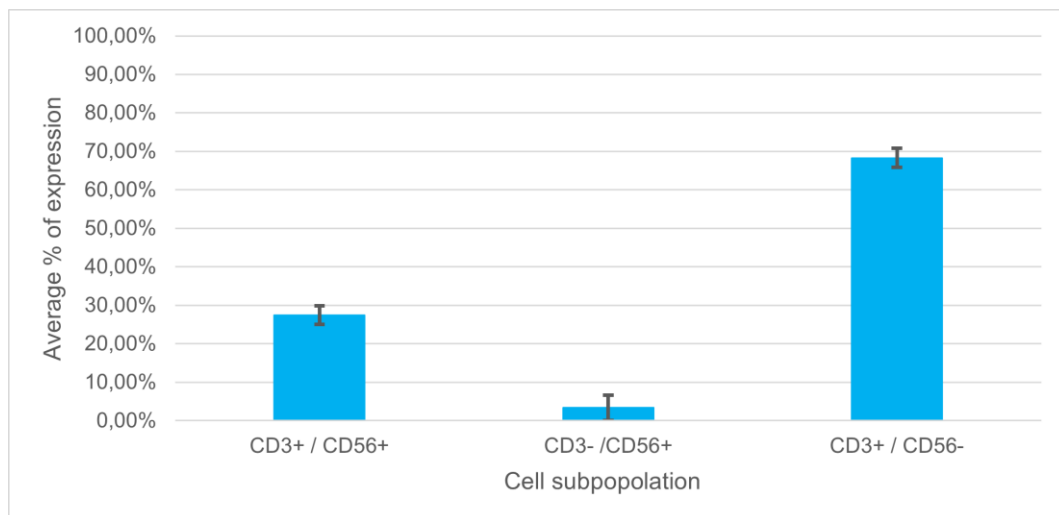


**Fig. 5. Average of the percentage of different cell subpopulations.** This graph shows the average percentage of different target cells within the samples (n=3).

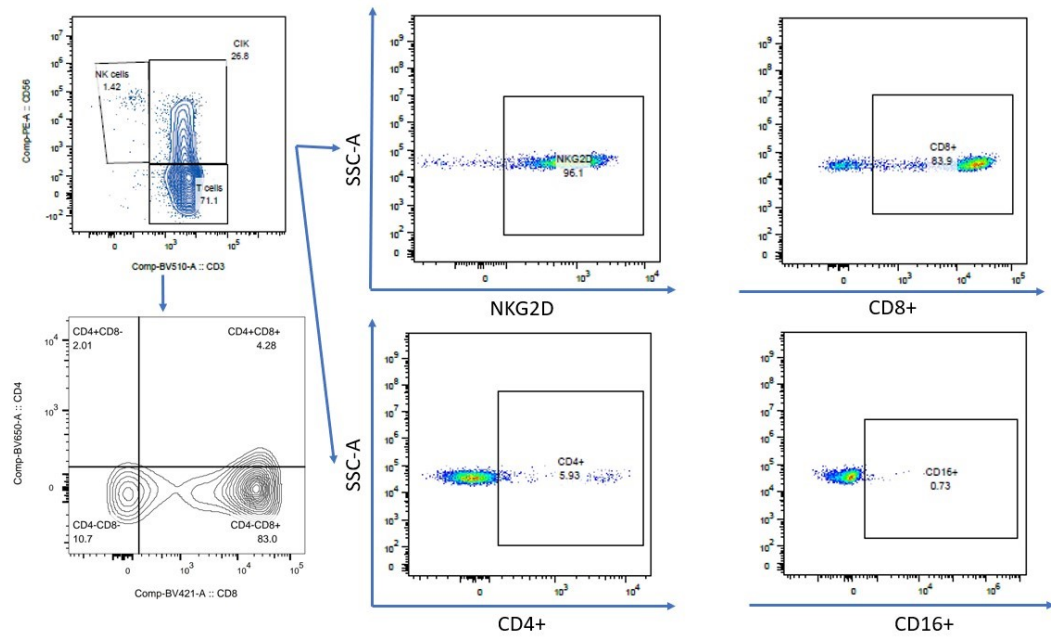


**Fig. 6. CIK cells' phenotypic characterization.** This figure shows the gating strategy used to characterize the phenotype of CIK cells (only one representative donor is shown).

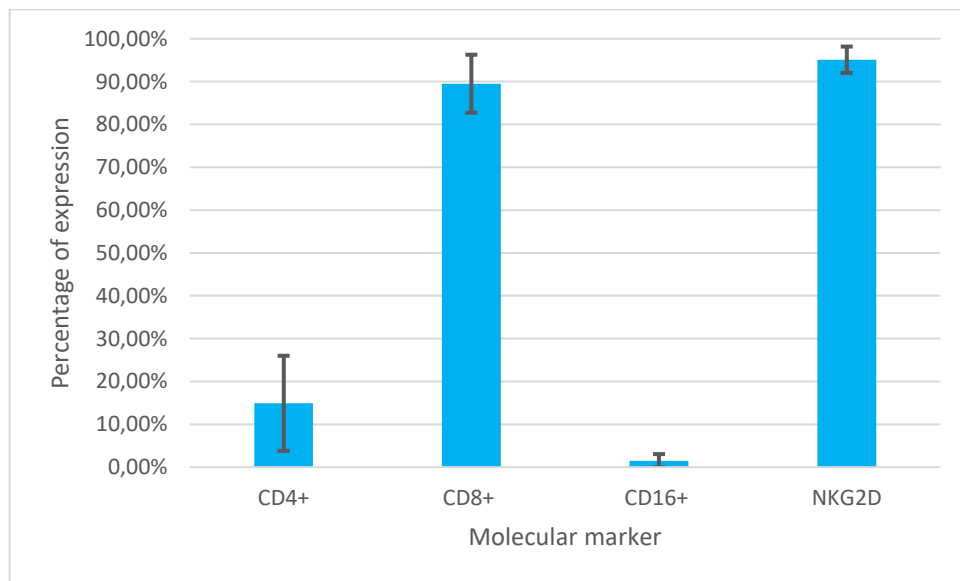


**Fig. 7. CIK cells' phenotype.** The image shows the average expression and the standard deviation of the different surface markers analyzed in the samples (n=3).

## 4.2 MCF-7 cells' phenotypic characterization

### 4.2.1 MCF-7 cells' gating strategy

MCF-7 breast cancer cells were phenotyped to test if there was an increase in the expression of NKG2D ligands after the treatment with different doses of ADU-



S100. MCF-7 cells were treated with 1  $\mu$ M, 5  $\mu$ M, 25  $\mu$ M and 100  $\mu$ M of ADU-S100, and their phenotype was checked after 24, 48, and 72 hours of treatment. NKG2D's ligands expression in the treated group was normalized to the expression in the untreated group. Singlets were isolated through the gating strategy mentioned in the material and methods. The background signal was isolated via the analysis of an unstained tube. The flow cytometry was done on single cells. Singlets population was isolated as stated in the material and methods. The flow cytometry showed that *in vitro* cultured cells were highly viable, with almost 90% of vitality, meaning that the treatment did not affect their vitality. MCF-7 cell population was isolated and characterized via the analysis of their specific size (FSC, Forward Scatter) and granularity (SSC, Side Scatter). The expression of the ligands of interest in the target population was assessed through multiple fluorescence-specific vs SSC-A plots.

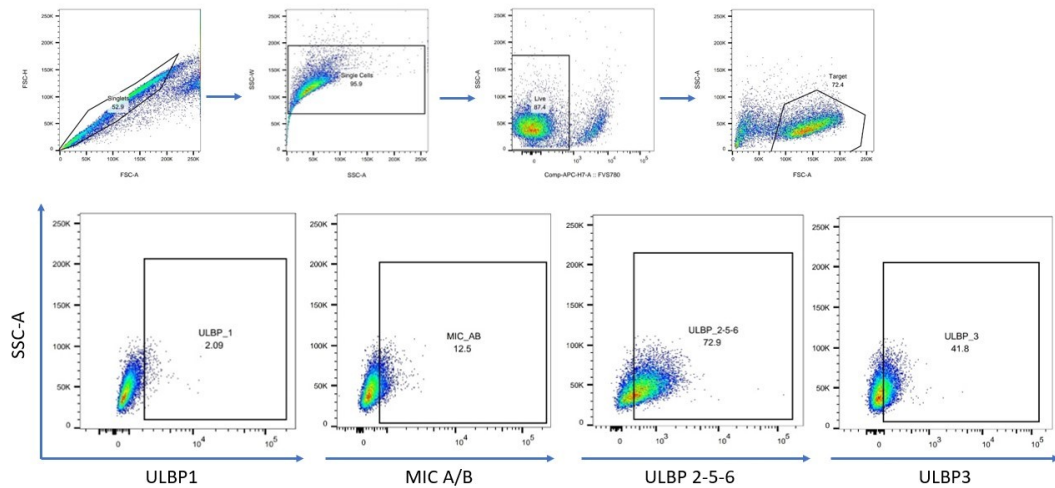


**Fig.8. MCF-7 cell's phenotypic characterization.** This figure shows the procedure used to identify MCF-7 cells and their phenotype.

#### 4.2.2 MCF-7 cells' phenotype

MCF-7 phenotype was obtained by flow cytometry after 24, 48, and 72 hours of treatment with different concentrations of ADU-S100. According to the FCM analysis, the treatment with ADU-S100 has no cytotoxic effect on MCF-7 cells, even at the highest concentration and after 72 hours.

MIC-A, MIC-B, ULBP1, ULBP2/5/6, and ULBP3 surface expression on MCF-7 cells was acquired as shown in Figure 8. The results were normalized to the control, which consisted of untreated MCF-7 cells. The treatment for 24 hours caused a significant change in the expression of all NKG2D's ligands, especially MIC A/B and ULBP-1. Changes in the expression of ULBP-1 seem to be directly correlated with ADU-S100 dosage since higher doses led to a higher expression while lower doses

led to a lower expression. The correlation between the dosage and the expression of the other surface markers of interest was not clear. Interestingly, after 48 hours of treatment, ADU-S100's effects started to vanish and, after 72 hours, the ligands' expression was even lower in comparison to the control. The only exception was ULBP-1, whose expression was still upregulated even after 72 hours of treatment. Based on these data we decided to treat MCF-7 cells with 100  $\mu$ M of ADU-S100 for 24 hours before performing the calcein-AM assay with CIK cells.

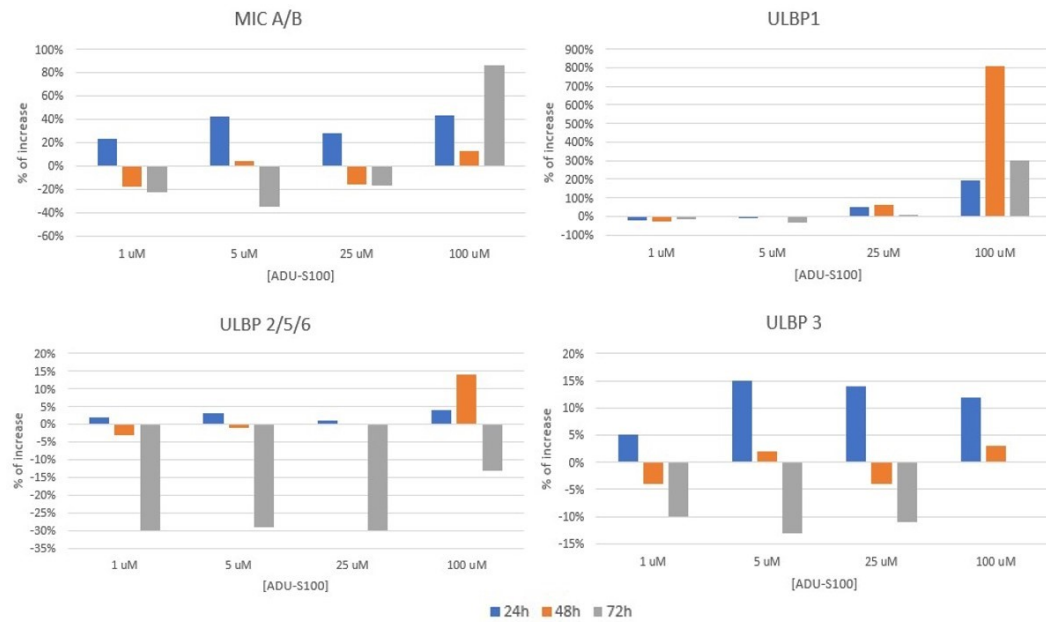


**Fig.9. MCF-7 cells' phenotype.** This image shows the percentage of the expression of NKG2D ligands compared to the untreated cells, after the treatment with different concentrations of ADU-S100 and at different time points (24, 48, and 72 hours).

### 4.3 Cytotoxic activity of CIK cells

The calcein-AM cytotoxic assay was performed on MCF-7 target cells seeded 48 hours before the assay and then treated with 100  $\mu$ M of ADU-S100 for 24 hours before the assay. Effector CIK cells were cultured according to a 14-day standard protocol (Schmidt-Wolf et al., 1991) as shown in Figure 3. CIK cells were cocultured with MCF-7 target cells for 6 hours to evaluate the cytotoxic effect of CIK cells against the target. Furthermore, it has been evaluated if there were any variations in CIK cells' cytotoxic activity following the combination between Trastuzumab (anti-HER-2 mAb) and the treatment with ADU-S100 in comparison to a control group which consisted of untreated MCF-7 cells supplemented with Rituximab (anti-CD19)

Unexpectedly, the treatment with ADU-S100 alone did not lead to a significant increase in the cytotoxic activity of CIK cells, as shown in Figure 10. Even at the

highest E:T ratio (50:1) CIK cells' cytotoxic activity was greater against untreated MCF-7 cells ( $79,31 \pm 34,50\%$ ) than against treated target cells ( $65,43 \pm 41,89\%$ ). The calcein-AM assay was also used to verify if the combination of ADU-S100 and trastuzumab could increase the antitumoral activity of CIK cells. ADU-S100-treated MCF-7 target cells were supplemented with Trastuzumab before the assay. Treated MCF-7 cells supplemented with rituximab were used as a negative control. As shown in Figure 10, at the highest E:T ratio (50:1) the combination of ADU-S100 and trastuzumab produced a significant increase in CIK cells' cytotoxic activity against HER-2<sup>+</sup> MCF-7 target cells ( $88,27\% \pm 37,41\%$ ) when compared to Rituximab supplemented treated MCF-7 cells ( $65,43\% \pm 41,89\%$ ).

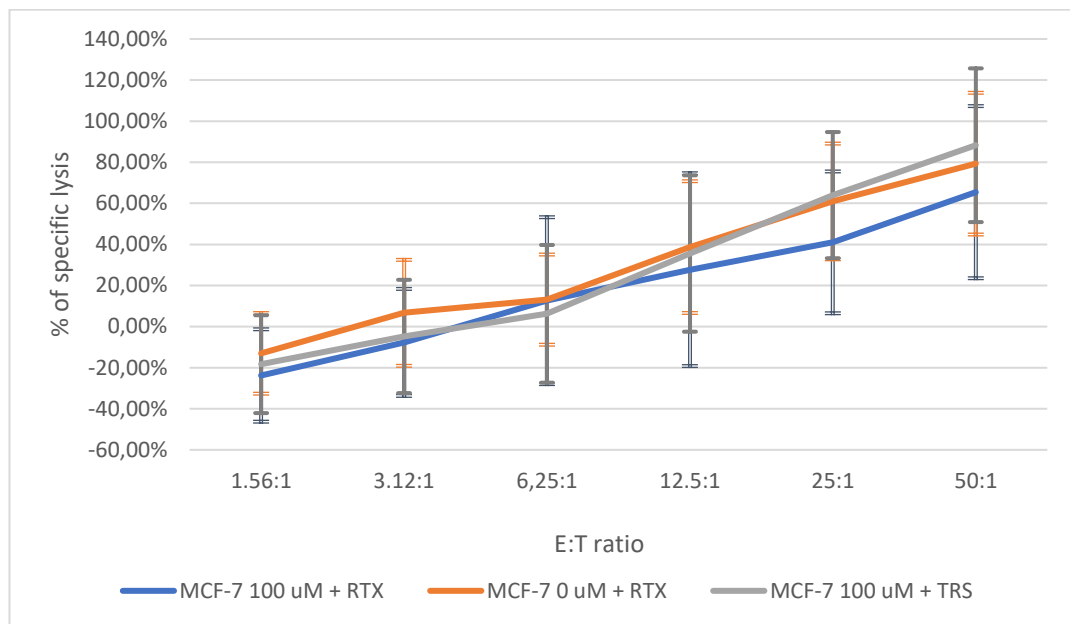


**Fig.10. Effects of ADU-S100 treatment on CIK cells' cytotoxic activity.** This image shows the effects of the different combinations between ADU-S100 and either Trastuzumab or Rituximab.

#### 4.3.1 Trastuzumab-mediated CIK cell retargeting

Since MCF-7 cells express HER2 receptors, we added Trastuzumab (anti-HER2 mAb) to increase CIK cells' cytotoxicity. In the single experiment performed, even at the highest E:T ratio, no significant difference between the antitumoral activity of CIK cells was observed after 6h of co-culture when CIK cells were combined with Trastuzumab ( $83,54\% \pm 41,68\%$ ) compared to when combined with the irrelevant antibody control Rituximab ( $79,31 \pm 34,50\%$ ). Further experiments are needed to elucidate this mechanism and the relationship between CD16 expression on CIK cells and the effectiveness of ADCC.

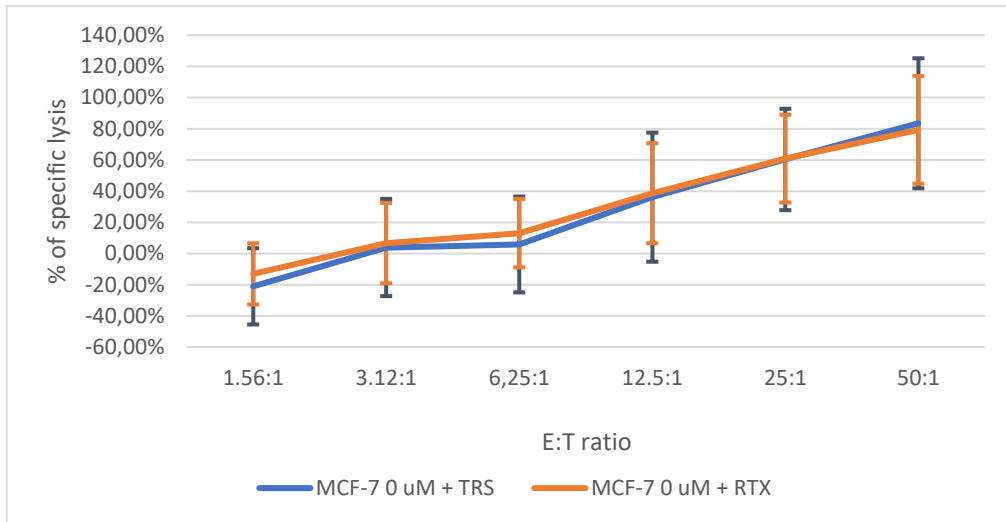


**Fig.11. Effects of trastuzumab-mediated CIK cell retargeting.**

## 5 DISCUSSION AND CONCLUSIONS

Cancer is the second leading cause of death worldwide. Traditional treatments present narrow therapeutical indexes and high toxicities, moreover, the ability of tumors to become resistant to most of them created the need for new therapeutical approaches. In this regard, the emerging field of ACT is showing great potential in the treatment of both solid and hematological tumors (Introna, 2017). ACT consists in the infusion of the patient's own immune cells which have been previously activated and/or genetically modified *ex vivo* to achieve anticancer activity. Among the different approaches for ACT, CIK cell therapy presents many advantages including easy availability, high proliferation rate, and MHC-unrestricted activity against malignant tissues but not against healthy tissues (Introna, 2017). CIK cells express NKG2D, a molecular receptor with the ability to bind multiple ligands, most of which are over-expressed after the activation of the cGAS-STING pathway in cancerous cells (Du et al., 2021). Since many tumors develop the ability to block the activation of the cGAS-STING pathway, with this experiment we tried to stimulate this process through the administration of ADU-S100, a c-di-AMP analog, and a STING agonist, to MCF-7 breast cancer cells. Furthermore, since CIK cells also express CD16, a molecular receptor involved in the process of Antibody-Dependent Cellular Cytotoxicity (ADCC), we tried to evaluate whether the combination of ADU-S100 with Trastuzumab, an anti-HER2 mAb, would lead to an increase in CIK cells' antitumor activity.

CIK cells were obtained from healthy donors' PBMCs and cultured following a 14-day standard protocol (Schmidt-Wolf et al., 1991). Their phenotype was evaluated by flow cytometry. MCF-7 breast cancer cells were cultured according to the protocol described in the materials and methods. MCF-7 breast cancer cells were cocultured with different concentrations of ADU-S100 for 24, 48, and 72 hours before performing the calcein-AM assay. Their phenotype was checked at different time points by flow cytometry to assess whether there has been an increase in the expression of the ligands of interest. The results showed that the treatment with 100  $\mu$ M ADU-S100 for 24 hours led to the upregulation of most of NKG2D's ligands of interest while the treatment with lower concentrations failed in activating the transduction cascade. The correlation between the dosage and the expression of the other surface markers of interest was not clear. Interestingly, after 48 hours of treatment, ADU-S100's effects started to vanish and, after 72 hours, the ligands' expression was even lower in comparison to the control.

The calcein-AM assay allowed us to evaluate the efficacy of both the treatment with ADU-S100 alone and in combination with Trastuzumab. Unexpectedly, the treatment with ADU-S100 alone did not lead to a significant increase in CIK cells'

cytotoxic activity. Even at the highest E:T ratio (50:1) CIK cells' cytotoxic activity was greater against untreated MCF-7 cells than against treated target cells. The correlation between ADU-S100 dosage and the upregulation of the expression of the ligands of interest is still not clear. Therefore, more *in vitro* experiments have to be performed in order to increase the number of samples and to clarify ADU-S100's action mechanism, its metabolism inside cancerous cells, and its role in the activation of the cGAS-STING pathway.

Since MCF-7 breast cancer cells express HER2 receptors, we hypothesized that the addition of Trastuzumab (anti-HER2 mAb) would have led to a significant increase in CIK cells' cytotoxic activity due to the activation of ADCC processes. In this experiment the combination of ADU-S100 and Trastuzumab did not lead to an increase in CIK cells' cytotoxic activity against HER-2<sup>+</sup> MCF-7 target cells when compared to Rituximab-supplemented treated MCF-7 cells, however, these results have to be confirmed by repeating this experiment. Furthermore, more *in vitro* experiments have to be performed to increase the number of samples analyzed and to understand the correlation between CD16a expression and the activation of ADCC induced by the recognition of Trastuzumab. The retargeting of CIK cells by the use of a clinically approved mAb could be promptly translated into clinical practice.

In conclusion, the treatment of cancer cells with ADU-S100 in combination with CIK cells is a promising ACT for the treatment of both solid and hematological tumors that is less challenging than T-cell genetic engineering, since CIK cells can be easily obtained and expanded *in vitro*. This study demonstrated that CIK cells are cytotoxic against MCF-7 breast cancer cells. Previous studies indicate that CIK cells express CD16a on their surface in a donor-dependent manner (Cappuzzello et al., 2016), however, since the samples analyzed in this study expressed CD16a at low levels the retargeting mediated by the addition of trastuzumab did not affect CIK cells cytotoxicity against MCF-7 target cells. In addition, the treatment of target cells with ADU-S100 for 24 hours led to an increase in the expression of NKG2D's ligands. However, in this study, we were unable to observe any correlation between the ligands' expression and the susceptibility of target cells to CIK cells. Since the antitumor effect of ADU-S100 has been demonstrated in multiple studies, more *in vitro* experiments need to be done in order to clarify the cellular mechanism of action of ADU-S100 and its applications in the field of immunotherapy.

## REFERENCES

1. Cancer Research Institute. (2023, February 9). *Adoptive Cell Therapy - Cancer Research Institute (CRI)*.  
<https://www.cancerresearch.org/treatment-types/adoptive-cell-therapy>
2. Schmeel, F. C., Schmeel, L. C., Gast, S., & Schmidt-Wolf, I. G. (2014). Adoptive Immunotherapy Strategies with Cytokine-Induced Killer (CIK) Cells in the Treatment of Hematological Malignancies. *International Journal of Molecular Sciences*, *15*(8), 14632–14648.  
<https://doi.org/10.3390/ijms150814632>
3. Introna, M. (2017). CIK as therapeutic agents against tumors. *Journal of Autoimmunity*, *85*, 32–44. <https://doi.org/10.1016/j.jaut.2017.06.008>
4. Du, H., Xu, T., & Cui, M. (2021). cGAS-STING signaling in cancer immunity and immunotherapy. *Biomedicine & Pharmacotherapy*, *133*, 110972. <https://doi.org/10.1016/j.biopha.2020.110972>
5. Chen, Q., Sun, L., & Chen, Z. J. (2016). Regulation and function of the cGAS–STING pathway of cytosolic DNA sensing. *Nature Immunology*, *17* (10), 1142–1149. <https://doi.org/10.1038/ni.3558>
6. Cappuzzello, E., Tosi, A., Zanovello, P., Sommaggio, R., & Rosato, A. (2016). Retargeting cytokine-induced killer cell activity by CD16 engagement with clinical-grade antibodies. *OncolImmunology*, *5*(8), e1199311. <https://doi.org/10.1080/2162402x.2016.1199311>
7. Esteves, A. M., Papaevangelou, E., Dasgupta, P., & Galustian, C. (2021). Combination of Interleukin-15 With a STING Agonist, ADU-S100 Analog: A Potential Immunotherapy for Prostate Cancer. *Frontiers in Oncology*, *11*. <https://doi.org/10.3389/fonc.2021.621550>
8. Bert, N. L., Lam, A. R., Ho, S., Shen, Y., Liu, M. M., & Gasser, S. (2014). STING-dependent cytosolic DNA sensor pathways regulate NKG2D ligand expression. *OncolImmunology*, *3*(6), e29259. <https://doi.org/10.4161/onci.29259>

9. Gao, X., Mi, Y., Guo, N., Xu, H., Xu, L., Gou, X., & Jin, W. (2017). Cytokine-Induced Killer Cells As Pharmacological Tools for Cancer Immunotherapy. *Frontiers in Immunology*, 8. <https://doi.org/10.3389/fimmu.2017.00774>
10. Schmidt-Wolf, I. G., Negrin, R. S., Kiem, H., Blume, K. G., & Weissman, I. L. (1991). Use of a SCID mouse/human lymphoma model to evaluate cytokine-induced killer cells with potent antitumor cell activity. *Journal of Experimental Medicine*, 174(1), 139–149. <https://doi.org/10.1084/jem.174>